

# Transient regulatory T cell ablation deters oncogene-driven breast cancer and enhances radiotherapy

Paula D. Bos,<sup>1,2</sup> George Plitas,<sup>4</sup> Dipayan Rudra,<sup>1,2</sup> Sue Y. Lee,<sup>1,2</sup> and Alexander Y. Rudensky<sup>1,2,3</sup>

<sup>1</sup>Howard Hughes Medical Institute and <sup>2</sup>Immunology Program, Sloan-Kettering Institute for Cancer Research; <sup>3</sup>Ludwig Center at Memorial Sloan-Kettering Cancer Center; and <sup>4</sup>Breast Service, Department of Surgery, Memorial Sloan-Kettering Cancer Center, New York, NY 10065

**Rational combinatorial therapeutic strategies have proven beneficial for the management of cancer. Recent success of checkpoint blockade in highly immunogenic tumors has renewed interest in immunotherapy. Regulatory T (T reg) cells densely populate solid tumors, which may promote progression through suppressing anti-tumor immune responses. We investigated the role of T reg cells in murine mammary carcinogenesis using an orthotopic, polyoma middle-T antigen-driven model in *Foxp3<sup>DTR</sup>* knockin mice. T reg cell ablation resulted in significant deterrent of primary and metastatic tumor progression. Importantly, short-term ablation of T reg cells in advanced spontaneous tumors led to extensive apoptotic tumor cell death. This anti-tumor activity was dependent on IFN- $\gamma$  and CD4<sup>+</sup> T cells but not on NK or CD8<sup>+</sup> T cells. Combination of T reg cell ablation with CTLA-4 or PD-1/PD-L1 blockade did not affect tumor growth or improve the therapeutic effect attained by T reg cell ablation alone. However, T reg cell targeting jointly with tumor irradiation significantly reduced tumor burden and improved overall survival. Together, our results demonstrate a major tumor-promoting role of T reg cells in an autochthonous model of tumorigenesis, and they reveal the potential therapeutic value of combining transient T reg cell ablation with radiotherapy for the management of poorly immunogenic, aggressive malignancies.**

## CORRESPONDENCE

Alexander Y. Rudensky:  
rudenska@mskcc.org

Abbreviations used: DT, diphtheria toxin; DTR, DT receptor; MMTV, murine mammary tumor virus; PyMT, polyoma middle T; rtTA, reverse tetracycline transactivator.

Cancer complexity generated by multiple genetic aberrations and intratumoral heterogeneity allows for resistance to single modality therapeutic approaches. Targeting multiple mechanisms that enable tumor growth by the design of rational combinatorial therapies has accounted for major advances in cancer treatment. Additionally, combinatorial strategies allow for lowering the dosage of the therapeutic agents, consequently reducing potential harmful side effects.

Over the last two decades, major efforts to mobilize the host immune system to treat different types of cancer have included vaccination and cytokine administration, yet the success of these attempts have been checkered. Targeting endogenous pathways of negative feedback regulation of immune cells has provided a major recent advance in cancer immunotherapy.

These mechanisms include cell-intrinsic downmodulation of activated T cell responsiveness and effector function by inhibitory receptors whose expression is induced upon acute or chronic T cell stimulation (Pardoll, 2012). Engagement of these receptors by their cognate ligands expressed by antigen-presenting cells, nonhematopoietic cells, or T cells themselves represents essential checkpoints of T cell activation and differentiation (Chen and Flies, 2013). Antibody-mediated blockade of interactions of two such receptors, CTLA-4 and PD-1 with their respective ligands CD80/CD86 and PD-L1/PD-L2, can facilitate anti-tumor immune responses in various experimental models, but only in combination with adoptive T cell therapy, vaccination, cryoablation, radiation, or chemotherapy (Mokyr et al., 1998; van Elsas et al., 1999;

P.D. Bos and G. Plitas contributed equally to this paper.  
D. Rudra's present address is Academy of Immunology and Microbiology, Institute of Basic Science, Pohang, Republic of Korea.

© 2013 Bos et al. This article is distributed under the terms of an Attribution-Noncommercial-Share Alike-No Mirror Sites license for the first six months after the publication date (see <http://www.rupress.org/terms>). After six months it is available under a Creative Commons License (Attribution-Noncommercial-Share Alike 3.0 Unported license, as described at <http://creativecommons.org/licenses/by-nc-sa/3.0/>).

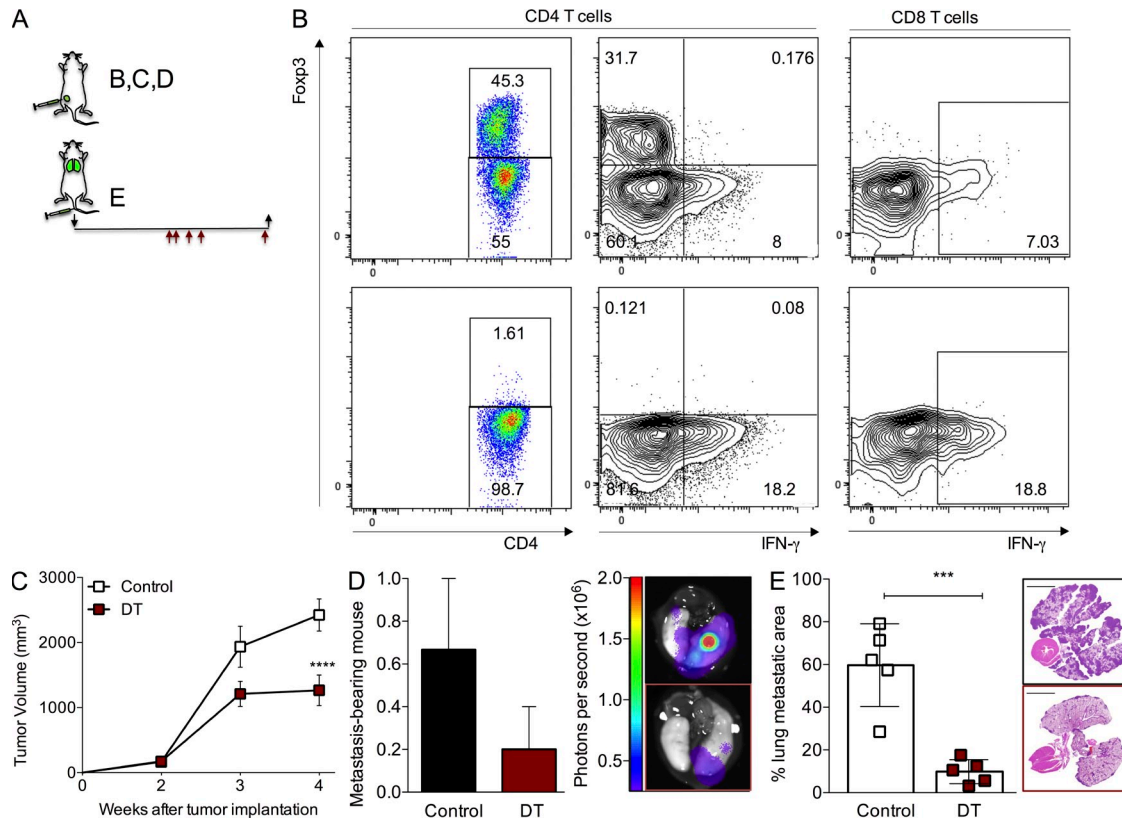


**Figure 1. Ablation of T reg cells affects the growth of fully established primary and lung metastatic tumors.** (A) Schematic of the experimental set up. Black arrows indicate day of tumor implantation ( $\downarrow$ ) and analysis ( $\uparrow$ ). Red arrows indicate regimen of DT treatment (days 14, 15, 17, 19, and 25 after tumor cell implantation). (B) Flow cytometric quantification of intratumoral CD4<sup>+</sup> Foxp3<sup>+</sup> T cells (left) and IFN- $\gamma$  production in T cells (right). Top: control; bottom: DT-treated. (C) Growth kinetics of orthotopic tumors in mice treated with 50  $\mu$ g/kg DT when tumors reached a volume of  $\sim$ 250 mm<sup>3</sup>. A representative of two independent experiments is shown;  $n = 5$  mice per group; \*\*\*\*,  $P < 0.0001$ . Error bars represent SEM. (D) Fraction and representative image of mice with detectable lung metastasis upon bioluminescence imaging of the dissected lungs from the group depicted in C. Error bars represent SEM. (E) Histological quantification and representative H&E staining image of the area of the lungs occupied with tumors in experimental lung colonization experiments; bars, 5,000  $\mu$ m; \*\*\*,  $P < 0.001$ . Error bars represent SD. Mice were injected with  $5 \times 10^5$  PyMT-derived cancer cells in the tail vein and treated with DT 2 wk after tumor injection with the schedule shown in A. P-values were calculated using ANOVA, followed by Bonferroni's post-hoc test (C) and Student's  $t$  test (E).

Hurwitz et al., 2000; Strome et al., 2003; Demaria et al., 2005; Waitz et al., 2012).

The aforementioned cell-intrinsic regulation of immune response is complemented by suppression of T cell-dependent inflammation by regulatory T (T reg) cells, whose differentiation and function is controlled by the transcription factor Foxp3. T reg cells constitute a major component of tumor-infiltrating lymphocytes in experimental mouse models of cancer and restrain tumor immunity. T reg cells also feature prominently in human malignancies, including breast cancer, where increased expression of Foxp3 among tumor-infiltrating lymphocytes correlates with poor prognosis and increased risk of recurrence (Facciabene et al., 2012). In mouse models of breast cancer, CD4<sup>+</sup> T cells have been suggested to play important roles in tumor progression and metastasis by inducing alternative activation of macrophages (DeNardo et al., 2009). T reg cells have been shown to promote metastasis by secreting extracellular signaling mediators such as RANK ligand (Tan et al., 2011). Akin to administration of CTLA-4 or PD-1 blocking

antibodies, T reg cell ablation results in regression of transplantable and chemically induced tumors via different mechanisms (Klages et al., 2010; Li et al., 2010; Teng et al., 2010). However, both checkpoint blockade and T reg cell ablation studies left open the question of whether these immunotherapeutic approaches are applicable to the treatment of established, poorly immunogenic oncogene-driven autochthonous tumors. Unlike melanomas or chemically induced tumors in which frequent immune-mediated rejection has led to the concept of immune editing (Schreiber et al., 2011), breast tumors are rarely spontaneously rejected in mice or humans. Human epithelial malignancies are most accurately modeled in mice by genetically engineered spontaneous cancer models, characterized by a driver mutation that facilitates the acquisition of further changes that result in invasive cancer, including the generation of a highly tolerogenic microenvironment (Willimsky and Blankenstein, 2005). Overcoming tumor-mediated immunosuppression in this setting would potentially expand the applicability of immunotherapy to a broad range of cancer types.

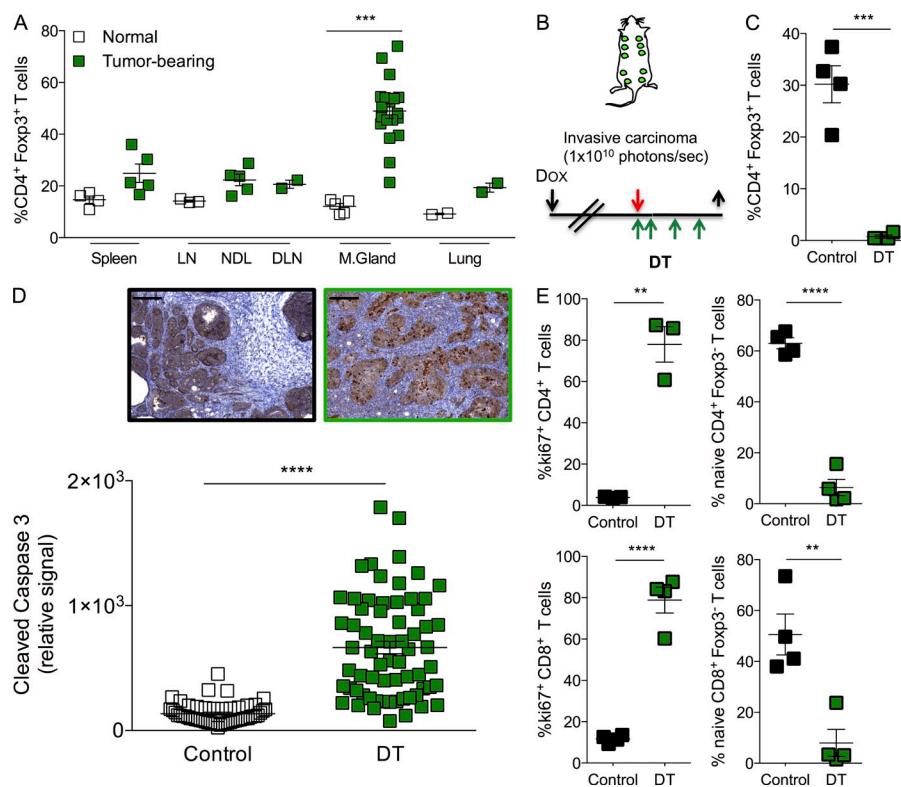


**Figure 2. Ablation of T reg cells results in tumor cell death in autochthonous breast tumors.** (A) Frequency of CD4<sup>+</sup> Foxp3<sup>+</sup> T reg cells in indicated organs of control (clear squares) and tumor-bearing (green squares) MMTV-rtTA; tet-O-PyMT (TOMT) mice. \*\*\*,  $P < 0.001$ . (B) Schedule of DT treatment in TOMT mice. Black arrows indicate days of doxycycline administration ( $\downarrow$ ) and analysis ( $\uparrow$ ). Red arrow indicates day the tumors reach mass emitting  $10^{10}$  photons per second. Green arrows indicate administration of DT. (C) Flow cytometric quantification of intratumoral CD4<sup>+</sup> Foxp3<sup>+</sup> T reg cells at end point (10 d after the first DT injection). A representative of at least three independent experiments is shown,  $n = 4$ ; \*\*\*,  $P < 0.001$ . (D) Histological quantification and representative images of tumor cell death by cleaved caspase-3 immunohistochemistry.  $n = 3-7$  mice per group; \*\*\*\*,  $P < 0.0001$ ; bars, 200  $\mu\text{m}$ . (E) Flow cytometric determination of the frequency of intratumoral proliferating (Ki67<sup>+</sup>) and naive (CD62L<sup>high</sup>CD44<sup>lo</sup>) CD4<sup>+</sup> and CD8<sup>+</sup> T cells. A representative of at least three independent experiments is shown;  $n = 3-4$  mice per group. Error bars represent SEM. \*\*,  $P < 0.01$ ; \*\*\*\*,  $P < 0.0001$ . NDL: nondraining LN; DLN: draining LN; M. Gland: mammary gland. P-values were calculated using Student's *t* test.

To address this important question, we explored the ability of T reg cell ablation to deter tumor progression in a stepwise mouse model of polyoma middle T (PyMT) oncogene-driven mammary carcinogenesis with high penetrance of lung metastasis (Guy et al., 1992). This transgenic model resembles the luminal type of human breast cancer (Lin et al., 2003) and is heavily infiltrated by innate immune cells and T lymphocytes. We found that transient ablation of T reg cells, employed as a single therapy, restrains oncogene-driven breast cancer progression and metastasis. This inhibition of tumor growth was dependent on IFN- $\gamma$  and CD4<sup>+</sup> T cells, but independent of NK and CD8<sup>+</sup> T cells. Although CTLA-4 and PD-1 checkpoint blockade did not enhance the anti-tumor effect of T reg cell ablation, the combination of T reg cell targeting and local radiotherapy resulted in a further marked reduction of tumor burden and in increased survival.

## RESULTS

### Therapeutic T reg cell ablation affects growth of large primary tumors and established lung metastasis

To determine the role of T reg cells in an oncogene-driven model of mammary tumorigenesis, we isolated carcinoma cells from C57BL/6 mice expressing a transgene encoding the PyMT oncogene under control of the murine mammary tumor virus (MMTV) promoter and implanted them in the knockin mice *Foxp3*<sup>DTR</sup>, which express the human diphtheria toxin (DT) receptor (DTR) under the control of the *Foxp3* locus (Kim et al., 2007). Orthotopic implantation of

only  $10^5$  tumor cells in the inguinal mammary gland of virgin female *Foxp3*<sup>DTR</sup> mice on a C57BL/6 background results in uniformly growing mammary tumors that metastasize to the lungs with complete penetrance in  $\sim 3-4$  wk. Using this strategy, we were able to evaluate tumor growth in large cohorts of mice with synchronous, rapidly progressing metastatic mammary tumors. We ablated Foxp3<sup>+</sup> T reg cells by injection of 50  $\mu\text{g}/\text{kg}$  of DT on days 1, 2, 4, 6, and 13 after tumor cell implantation, and we observed significant reduction in tumor growth and incidence of lung metastasis (unpublished data). Flow cytometric analysis of lymphocyte populations isolated from enzymatically dissociated tumors demonstrated that the extent of T reg cell ablation was  $>99\%$  (Fig. 1 B). We also found expansion and activation of CD4<sup>+</sup> and CD8<sup>+</sup> T cell subsets based on the increased expression of Ki67 and CD44 and decreased levels of CD62L (unpublished data). In addition, the proportion of CD4<sup>+</sup> and CD8<sup>+</sup> T cells expressing IFN- $\gamma$  and TNF was markedly augmented (Fig. 1 B and not depicted). Furthermore, we also observed an increase in immature myeloid cells (unpublished data). Next, we sought to test the effect of T reg cell ablation on established tumors that reached exponential growth ( $\sim 250 \text{ mm}^3$ ; Fig. 1 A). DT treatment of *Foxp3*<sup>DTR</sup> mice with large tumors resulted in significant reduction of tumor burden (Fig. 1 C). In addition, the incidence and size of lung metastasis in mice bearing large tumors was reduced upon depletion of T reg cells (Fig. 1 D). The observed reduction in lung metastatic burden could have been secondary to reduced primary tumor volume in



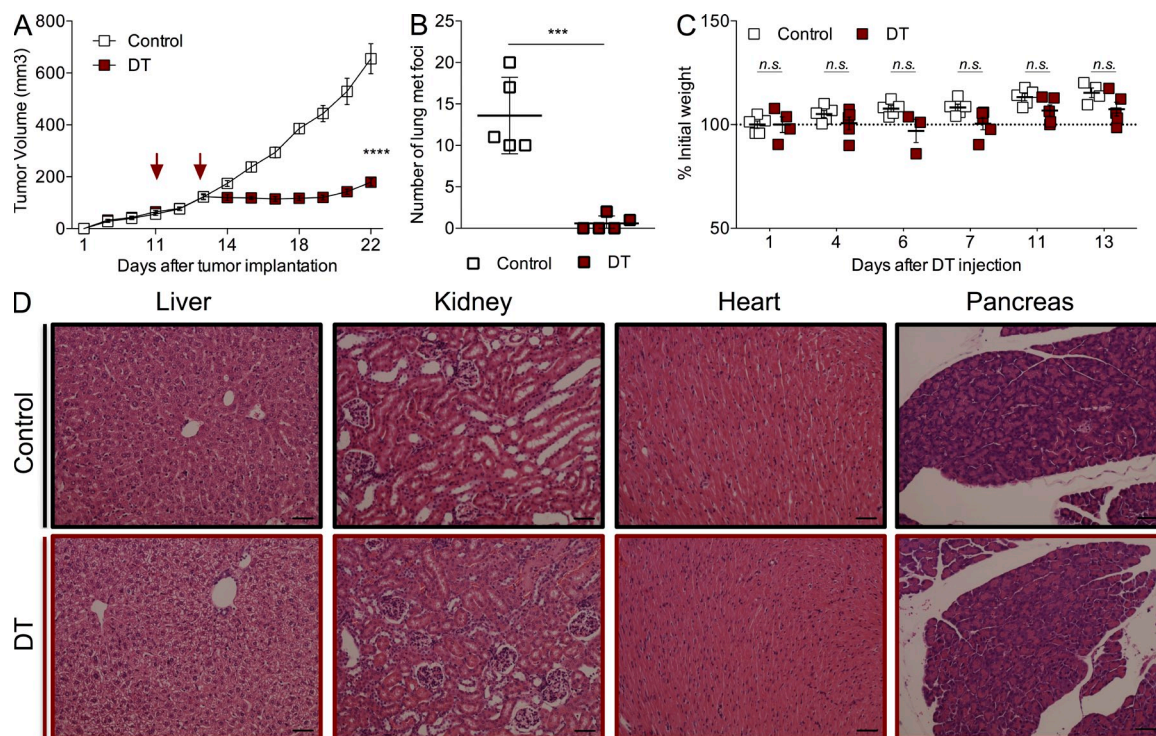


**Figure 3. Transient T reg cell ablation is sufficient for inhibition of tumor growth without significant side effects.** (A) Growth kinetics of orthotopically implanted tumors treated with 25 µg/kg DT at the indicated times; \*\*\*\*,  $P < 0.0001$ . Error bars represent SEM. (B) Number of metastatic nodules present on the lung surface upon examination under a dissection microscope; \*\*\*,  $P < 0.001$ . Error bars represent SEM. (C) Body weight fluctuations represented as percentage of weight at the time of initial DT administration. Error bars represent SEM. (D) Representative histological images of liver, kidney, heart, and pancreas from control and DT-treated mice 2 wk after treatment.  $n = 3-5$  mice per group, representative of at least three independent experiments. Bars, 50 µm. P-values were calculated using ANOVA followed by Bonferroni's post-hoc test (A) and Student's *t* test (B).

DT-treated animals because metastatic load is proportional to primary tumor size (Heimann and Hellman, 2000; Minn et al., 2007). To investigate whether the beneficial effect of T reg cell ablation on lung metastasis in these experiments was independent of the diminished primary tumor growth, we treated animals with DT after establishment of lung metastasis 2 wk after tail vein inoculation of  $5 \times 10^5$  PyMT cells (Fig. 1 A). Analysis performed 2 wk after DT injection showed that tumor burden in the lungs was markedly reduced as determined by histological quantification of tumor areas in lung sections, demonstrating a pronounced direct effect of T reg cell ablation on the disseminated tumors (Fig. 1 E). These studies demonstrate that T reg cell ablation is therapeutic not only for newly formed but also for large, rapidly growing primary mammary tumors and fully established lung metastasis.

#### T reg cell ablation results in tumor cell death in spontaneously developing oncogene-driven mammary tumors

The potent restraint of cancer progression and metastasis in the orthotopic transplantation model of breast carcinogenesis observed upon T reg cell ablation raised a question of whether it can be efficacious when applied to genetically induced oncogene-driven tumors. To address this issue, we introduced the *Foxp3<sup>DTR</sup>* allele into mice coexpressing PyMT oncogene together with a luciferase reporter regulated by a doxycycline-inducible

promoter and reverse tetracycline-controlled transactivator under the MMTV promoter (MMTV–reverse tetracycline transactivator [rtTA]; tet-O-MT:IRES:Luc or TOMT; Podsypanina et al., 2008). Upon doxycycline administration, these mice developed tumors in all mammary glands. Analysis of tumor-infiltrating lymphocytes showed that T reg cells were highly enriched within the CD4<sup>+</sup> T cell subset (Fig. 2 A). We allowed mice to develop large invasive carcinomas that emitted a photon flux of  $10^{10}$  photons per second and set the time point of analysis at 10 d after the initial dose of DT (Fig. 2 B). At that time, the mice are fully active and do not present any signs of morbidity despite sustained T reg cell ablation (Fig. 2 C). Because asynchronous and slow tumor growth in TOMT mice precludes the accurate evaluation of the effect of T reg cell ablation on growth kinetics, we analyzed expression of cleaved caspase-3 in cancer cells, a marker of apoptotic death, as a means to assess the consequence of T reg cell ablation on tumor viability. We observed a remarkable increase in apoptosis of tumor cells in mice treated with DT compared with control mice injected with PBS (Fig. 2 D). Concomitantly, we observed significant expansion and activation of intratumoral CD4<sup>+</sup> and CD8<sup>+</sup> T cells in T reg cell–depleted mice (Fig. 2 E). These results indicate that T reg cells represent a major cellular mechanism facilitating tumor progression by maintaining cancer cell viability in this experimental model of oncogene-driven breast cancer.

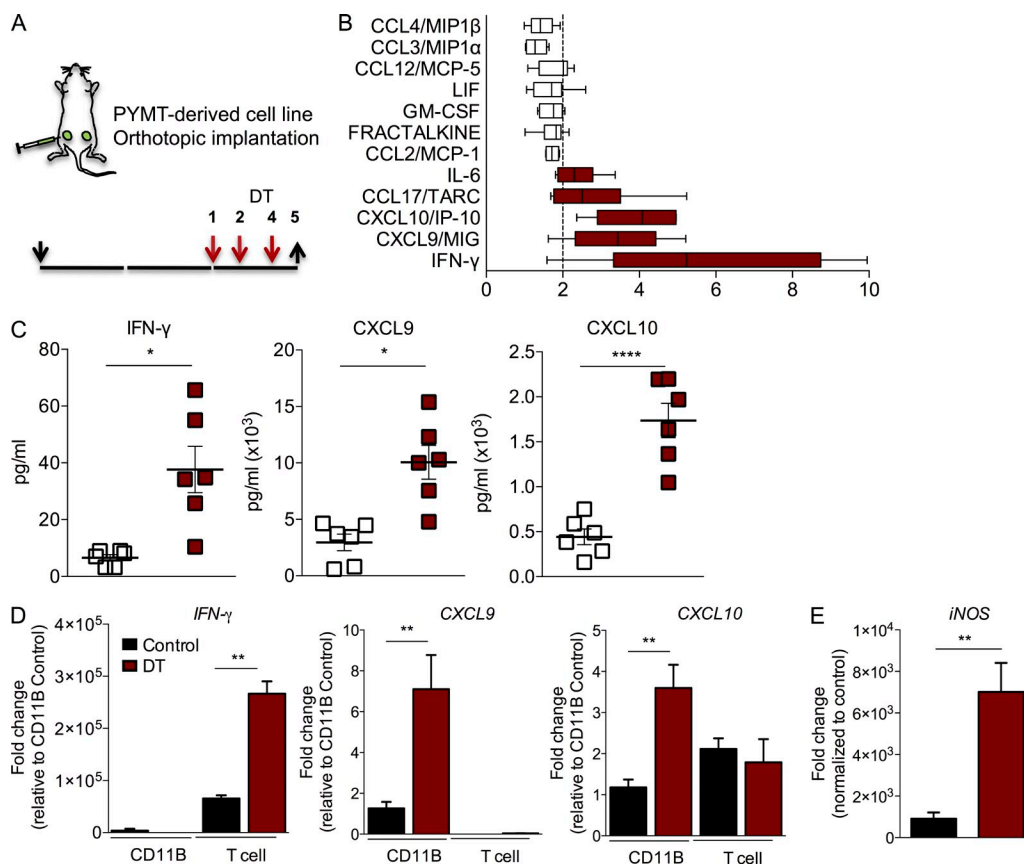


**Figure 4. T reg cell ablation results in increased production of IFN- $\gamma$  and IFN- $\gamma$ -dependent changes.** (A) Scheme of DT treatment. Black arrows indicate day of tumor implantation ( $\downarrow$ ) and analysis ( $\uparrow$ ). Red arrows indicate regimen of DT treatment. (B) Significant changes in chemokine and cytokine levels in tumor lysates from DT-treated mice analyzed by cytokine/chemokine array. X-axis represents fold change compared with control. A representative of two independent experiments is shown,  $n = 3$  mice with two tumors each analyzed per group. Error bars represent minimum and maximum. (C) Analysis of IFN- $\gamma$ , CXCL9, and CXCL10 protein levels in tumor lysates from control and DT-treated mice using multiplex bead assay. The data are shown as concentrations of indicated factors (pg/ml). A representative of two independent experiments is shown. \*,  $P < 0.05$ ; \*\*\*\*,  $P < 0.0001$ . Error bars represent SEM. (D) qPCR analysis of cell type-specific expression of IFN- $\gamma$ , CXCL9, and CXCL10. RNA was extracted from CD45 $^{+}$  TCR- $\beta^{-}$  CD11B $^{+}$  Gr1 $^{-}$  or CD45 $^{+}$  TCR- $\beta^{+}$  CD11B $^{-}$  FACS-purified cells;  $n = 3$  mice per group; \*\*,  $P < 0.01$ . Error bars represent SEM. (E) qPCR analysis of *iNOS*, consistent with classical polarization of myeloid cells;  $n = 3$  mice per group. Error bars represent SEM. \*\*,  $P < 0.01$ . P-values were calculated using Student's *t* test.

### Transient T reg cell ablation is sufficient to achieve significant reduction in tumor burden

To minimize the potential side effects of T reg cell ablation and test whether continuous ablation was required to achieve the observed reduction in orthotopic tumor growth, we decided to limit the dose and frequency of the DT administration. We gave tumor-bearing animals only two doses of DT (25  $\mu$ g/kg) once tumors reached a volume of  $\sim 100$  mm $^3$ . This treatment regimen allows for efficient (>99%) yet transient T reg cell ablation with minimal morbidity (slight short-term weight loss followed by a quick recovery; Fig. 3 C) and no gross organ immunopathology evaluated by histological examination 2 wk after DT (Fig. 3 D). Remarkably, despite lack of pronounced generalized immunopathology, this brief ablation of T reg cells significantly hindered primary tumor growth (Fig. 3 A) and resulted in the almost complete disappearance of metastatic tumor nodules in the lungs (Fig. 3 B). These experiments demonstrate that efficient ablation of

T reg cells for a very short period of time provides therapeutic benefit similar to that of persistent ablation, while reducing the dangerous side effects to a bare minimum.

### T reg cell ablation promotes a tumor-suppressive microenvironment

T reg cells could be beneficial to cancer cell growth and tumor progression in several ways. On one hand, they can suppress components of the adaptive immune system providing protection against antigen-specific tumor cell killing. On the other hand, they can modulate components of the tumor microenvironment that may directly or indirectly promote tumor progression. To better understand the early changes taking place in the tumor milieu upon T reg cell ablation, we performed a protein array of 66 cytokines and chemokines on tumor lysates prepared on day 5 after DT administration to evaluate early changes in these soluble mediators (Fig. 4 A). Comparison of control and DT-treated tumor lysates revealed

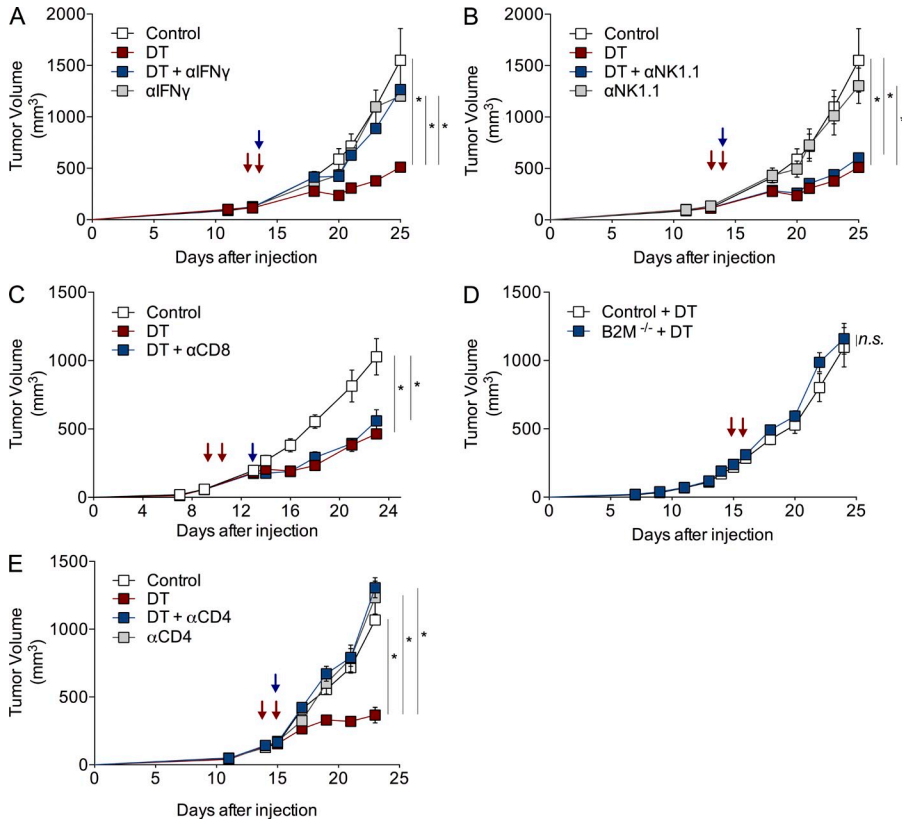


**Figure 5. Anti-tumor effect of T reg cell ablation requires CD4<sup>+</sup> T cells and IFN- $\gamma$ , but not CD8<sup>+</sup> or NK cells.** (A–E) Growth kinetics of orthotopically implanted tumors in mice treated with 25  $\mu$ g/kg DT at indicated times, in combination with 1 mg IFN- $\gamma$  (A) or 300  $\mu$ g NK1.1 antibody (B) on day 10, 250  $\mu$ g CD8 antibody on day 13 (C), or 100  $\mu$ g CD4 antibody on day 10 (E). Blue arrows indicate antibody treatment. Red arrows indicate DT injection. (D) Tumor growth kinetics of control or DT-treated  $\beta 2M^{-/-}$  *Foxp3<sup>DTR</sup>* mice. A representative of two independent experiments is shown;  $n = 5$  mice per group. Error bars represent SEM. \*,  $P < 0.05$ . P-values were calculated using ANOVA followed by Bonferroni’s post-hoc test.

significant increments in 12 cytokines, although only 5 of them increased above a twofold threshold (Fig. 4 B). The most prominent increase was observed in IFN- $\gamma$ , a proinflammatory cytokine with potent anti-tumor effects, followed by CXCL9 and CXCL10 (Fig. 4 C). These two chemokines are produced by several cell types in response to IFN- $\gamma$  and serve as chemoattractant for CXCR3-expressing leukocytes, most notably Th1 and NK cells, but also monocytes. To validate these observations and determine the source of each cytokine, we isolated T cells (CD45<sup>+</sup>CD3<sup>+</sup>CD11B<sup>-</sup>Gr1<sup>-</sup>) and myeloid cells (CD45<sup>+</sup>CD3<sup>-</sup>CD11B<sup>+</sup>Gr1<sup>-</sup>) from an independent group of control and DT-treated tumors by fluorescence activated cell sorting. Using primer-specific semiquantitative PCR, we determined their mRNA levels in these two populations. We observed that IFN- $\gamma$  was produced in the T cell compartment and increased significantly upon T reg cell ablation, whereas CXCL9 and CXCL10 were significantly increased in the myeloid compartment upon DT treatment, likely as a response to IFN- $\gamma$  (Fig. 4 D). Because IFN- $\gamma$  is a potent classic activator of macrophages, we quantified the mRNA levels of iNOS, a prototypical IFN- $\gamma$ -induced effector molecule of M1 polarized macrophages. We observed a marked up-regulation of iNOS expression in the myeloid cell compartment upon T reg cell ablation (Fig. 4 E). Altogether, our results suggest that T reg cell ablation leads to a strong IFN- $\gamma$ -dominated tumor milieu that can promote the anti-tumor responses of Th1, NK, and CD8<sup>+</sup> T cells or generation of M1 macrophages.

**Tumoricidal effects are mediated via IFN- $\gamma$ , but not CD8<sup>+</sup> T cells or NK cells**

Given the predominance of IFN- $\gamma$  in T reg cell-depleted tumors, we sought to evaluate its role in the observed delayed tumor progression. Thus, we injected tumor-bearing *Foxp3<sup>DTR</sup>* mice with 1 mg IFN- $\gamma$  neutralizing antibody alone or in combination with DT. Although IFN- $\gamma$  antibody treatment alone did not have an impact on tumor growth in control mice, IFN- $\gamma$  antibody almost completely abolished the effect of DT-mediated T reg cell ablation on tumor growth (Fig. 5 A). Next, we wanted to determine whether the anti-tumoral effect was mediated through cytotoxic T or NK cells. To test this, we ablated T reg cells in the presence of NK- or CD8-depleting antibodies. NK cell depletion using NK1.1 antibody did not have a detectable effect on growth of control or T reg cell-depleted tumors (Fig. 5 B). In addition, administration of CD8-depleting antibody during the course of T reg cell ablation did not affect the resulting tumor growth reduction (Fig. 5 C). To corroborate this finding, we made use of *Foxp3<sup>DTR</sup>* mice lacking  $\beta 2$ -microglobulin, which are required for MHC class I expression and proper maturation of CD8<sup>+</sup> T cells (Gasteiger et al., 2013). In agreement with antibody-mediated depletion, T reg cell ablation in control or DT-treated *Foxp3<sup>DTR</sup>*  $\beta 2M^{-/-}$  mice resulted in comparable detriment of tumor progression and indistinguishable tumor growth profiles (Fig. 5 D). In contrast, when CD4<sup>+</sup> cells were depleted from the DT-treated tumors, there was a pronounced attenuation in the T reg cell ablation-mediated anti-tumor effect (Fig. 5 E).



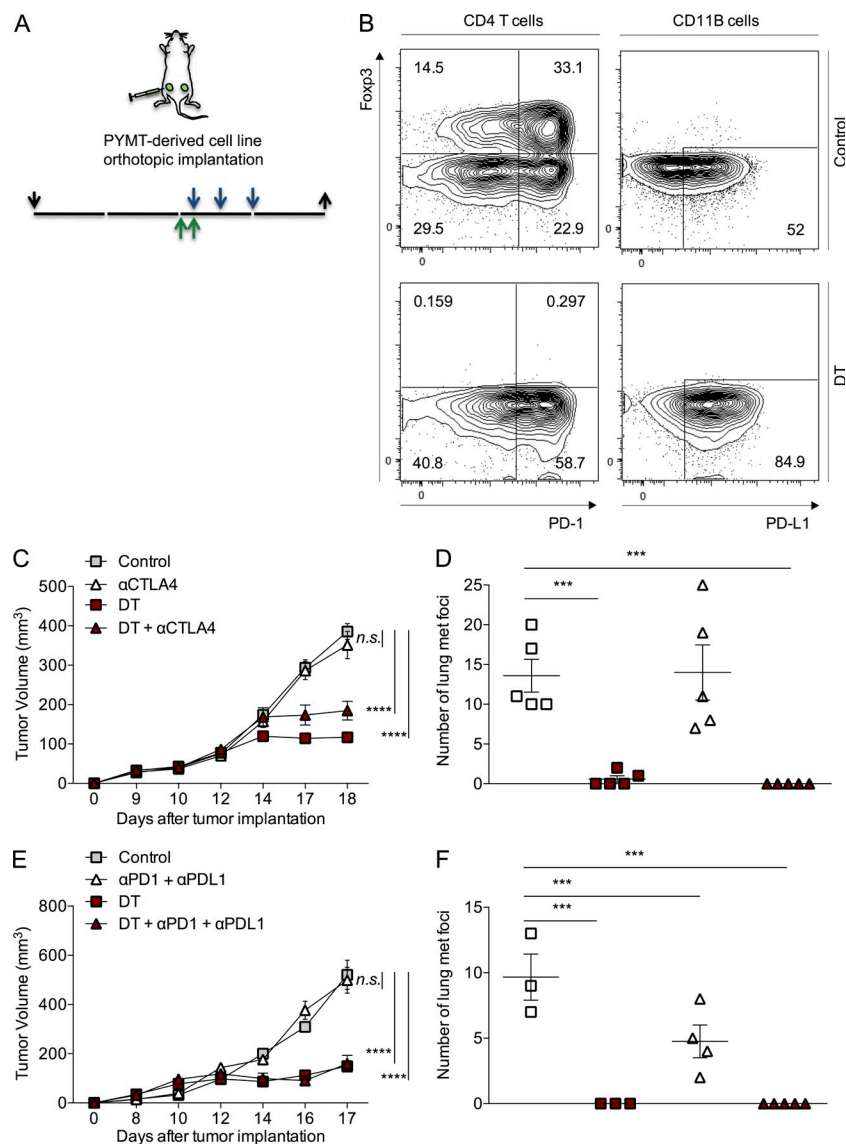


**Figure 6. Checkpoint blockade does not affect oncogene-driven tumor growth and lung metastasis, nor does it cooperate with T reg cell ablation.** (A) Diagram of experimental set up. Green arrows indicate injection of 25  $\mu\text{g}/\text{kg}$  DT, blue arrows indicate injection of specific antibody, and black arrows indicate day of tumor implantation ( $\downarrow$ ) and analysis ( $\uparrow$ ). (B) Expression of PD-1 and PD-L1 on CD4<sup>+</sup> T cells (left) and CD11B<sup>+</sup> cells (right) in control (top) and DT-treated tumors (bottom) assessed by flow cytometry. (C and E) Tumor growth kinetics of orthotopically implanted PyMT-driven mammary carcinomas. Mice were treated with 0.1 mg CTLA-4 (C) or 0.25 mg PD-1 + 0.1 mg PD-L1 antibodies (E) on days 0, 3, and 6 after tumors reached a volume of  $\sim 100$  mm<sup>3</sup> after implantation of  $10^5$  tumor cells in the mammary fat pad of 6–8-wk-old female virgin mice. 25  $\mu\text{g}/\text{kg}$  DT was injected intravenously on days  $-1$  and  $0$  of initial antibody treatment. One representative of two independent experiments,  $n = 5$  mice per group. (D and F) Number of metastatic nodules present on the lung surface quantified upon examination under a dissecting microscope. Error bars represent SEM. \*\*\*,  $P < 0.001$ ; \*\*\*\*,  $P < 0.0001$ . P-values were calculated using ANOVA followed by Bonferroni's post-hoc test.

Together, these results indicate that NK and CD8<sup>+</sup> T cells are not necessary for the anti-tumor effect of T reg cell ablation, which is dependent on CD4<sup>+</sup> T cells and requires IFN- $\gamma$ . In addition, these observations suggest that NK and CD8<sup>+</sup> T cells are dispensable as sources of IFN- $\gamma$ .

#### Checkpoint blockade does not improve the effect of T reg cell ablation on mammary tumor progression

Encouraged by the potent anti-tumor effect achieved via T reg cell ablation, we looked for potentially cooperative therapeutic approaches. Highly expressed on activated and chronically stimulated (“exhausted”) effector cells, CTLA-4, PD-1, and its ligand PD-L1 are also present in high amounts on T reg cells (Pardoll, 2012), and their antibody-mediated inhibition has proven a viable immunotherapeutic strategy to treat solid tumors in recent preclinical studies and clinical trials. Therefore, immune checkpoint blockade jointly with T reg cell depletion could potentially further promote the effector

response of newly recruited T cells in addition to reversing the exhausted state of preexisting tumor-infiltrating T cells.

In support of this concept, tumor-infiltrating lymphocytes in T reg cell-depleted tumors exhibited a marked increase in the expression of the PD-1 receptor on effector T cells. Additionally, expression of the PD-L1 ligand was increased on both T cells and myeloid cells (Fig. 6 B and not depicted). Thus, we sought to test whether combination with CTLA-4 or PD-1 checkpoint blockade could enhance the therapeutic effect of T reg cell ablation in our oncogene-driven breast cancer model. First, we examined the effects of targeting the CTLA-4 or PD-1/PD-L1 inhibitory pathways with blocking antibodies of corresponding specificity administered on days 0, 3, and 6 after tumors reached a volume of  $\sim 100$  mm<sup>3</sup>. Blockade of either one of these pathways by CTLA-4 or PD-1 or PD-L1 or a combination of PD-1 and PD-L1 antibodies had no significant effect on the growth of PyMT-driven orthotopic tumors (Fig. 6, A, C, and E; and

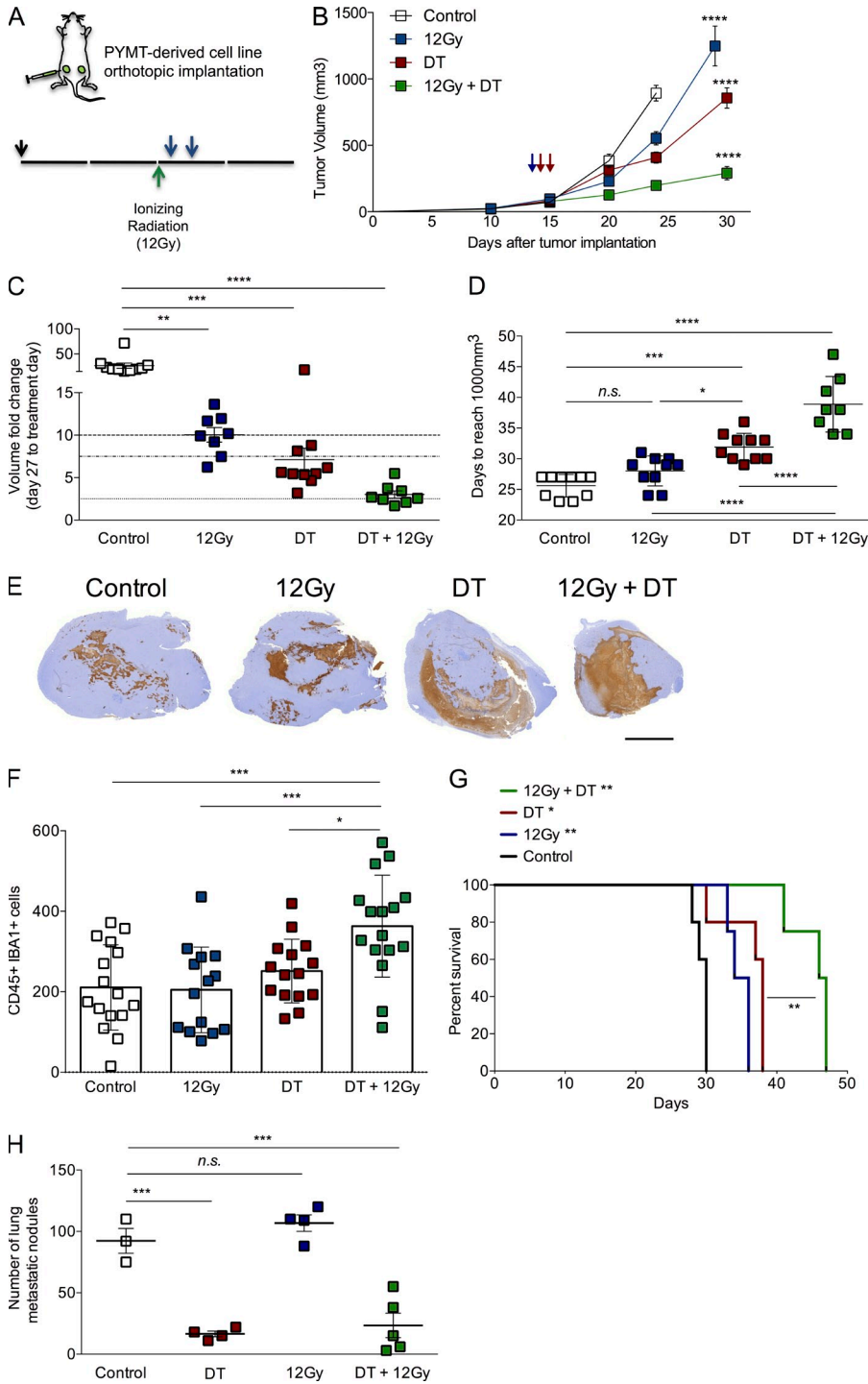


**Figure 7. T reg cell ablation improves the effect of ionizing radiation on tumor growth.** (A) Scheme of treatment. 12Gy of ionizing radiation was delivered in a single fraction when tumors reached a volume of ~100 mm<sup>3</sup> (green arrow), followed by two i.v. injections of 25 μg/kg DT (blue arrows). Orthotopic tumor transplantation is indicated by a black arrow (↓). (B) Tumor growth kinetics in mice subjected to radiation alone, DT-mediated T reg cell ablation alone, a combination of both, or no treatment. \*\*\*\*,  $P < 0.0001$ . (C) Analysis of fold change increase in tumor size for each group at day 27 after initial treatment. \*\*,  $P < 0.01$ ; \*\*\*,  $P < 0.001$ ; \*\*\*\*,  $P < 0.0001$ . (D) Day at which a given tumor reaches a volume of at least 1,000 mm<sup>3</sup>. n.s., not significant; \*,  $P < 0.05$ ; \*\*\*,  $P < 0.001$ ; \*\*\*\*,  $P < 0.0001$ . (E) Representative images of histological staining with cleaved Caspase 3, depicting the area of apoptotic cells observed in each individual tumor.  $n = 3-5$  mice per group. Bar, 5,000 μm. (F) Histological assessment of the number of CD45<sup>+</sup> IBA1<sup>+</sup> cells in representative viable regions of the tumor. \*,  $P < 0.05$ ; \*\*\*,  $P < 0.001$ . (G) Survival analysis of mice in each of the animal groups described above. \*,  $P < 0.05$ ; \*\*,  $P < 0.01$ . (H) Time-matched quantification of metastatic nodules in lungs from mice in each group. \*\*\*,  $P < 0.001$ . A representative of two independent experiments is shown;  $n = 5$  mice per group. Error bars represent SEM. P-values were calculated using ANOVA followed by Bonferroni's post-hoc test.

not depicted). Of note, lung metastatic burden measured by enumerating tumor nodules on the lung surface was diminished by half upon the blockade of PD-1/PD-L1 but not CTLA-4 signaling (Fig. 6, D and F). A combination of DT with CTLA-4 antibody or with PD-1 and PD-L1 antibodies did not enhance the effect of T reg cell ablation alone on primary tumor progression (Fig. 6, C and E). DT treatment almost completely eliminated the appearance of metastatic

nodules in the lungs (Fig. 6, D and F). Thus, we were unable to evaluate the potential synergistic effects of T reg cell ablation and PD-1/PD-L1 blockade in this experimental setup, although the latter did have a beneficial effect as monotherapy (Fig. 6 F). Our observations suggest that efficient targeting of T reg cells is necessary and sufficient to achieve an effective immunotherapeutic response to the growing tumor in this model of oncogene-dependent cancer.



### Transient T reg cell ablation significantly improves the outcome of ionizing radiation therapy

Given that no advantage was offered by a combination with checkpoint blockade, the leading immune-based strategy in the treatment of metastatic tumors, we evaluated the ability of T reg cell ablation to increase the efficacy of ionizing radiation aimed at inhibiting proliferation and inducing cell death. Local radiotherapy, widely used in the management of breast cancer, has the potential to synergize with T reg cell ablation in several ways. First, T reg cells are markedly more resistant to radiation than conventional T cells, and increased T reg/T effector cell ratio upon radiotherapy may reduce its efficacy (Komatsu and Hori, 2007; not depicted). Second, radiation can modulate immune response through the release of tissue damage factors that attract immune cells, stimulate antigen presentation, increase tumor antigen pool, and sensitize cancer cells to immune-mediated killing. Lastly, the high rate of cancer cell death resulting in tumor debulking contributes to a decrease in persistent antigens that can induce tolerance (Drake, 2012; Coussens et al., 2013).

First, we compared the two most commonly used doses of experimental local tumor irradiation, 7.5Gy and 12Gy, and found that the latter reduced the size of the tumors by 50% in the 2 wk after treatment (unpublished data). Thus, we stereotactically delivered 12Gy radiation to mice bearing  $\sim 100 \text{ mm}^3$  (and  $250 \text{ mm}^3$ ; unpublished data) bilateral tumors, and we depleted T reg cells by administering DT on days 1 and 2 after radiation, before rise in T reg cell/T effector cell ratio (Fig. 7 A and not depicted). The combination of radiation with transient T reg cell ablation affected the tumor growth much more significantly than either treatment alone, with the most pronounced cooperative effects observed by the end of the experiment. By that time, control and single therapy groups of mice were euthanized due to heavy tumor burden before tumors in the combination treatment group reached exponential growth phase (Fig. 7 B). During the first 2 wk of the experiment, volumes of control tumors had increased 50-fold, irradiated tumors 10-fold, T reg cell-depleted tumors 7.5-fold, and tumors treated with the combination had only increased  $\sim 2.5$ -fold (Fig. 7 C). When we measured the mean time tumors needed to reach a volume of  $\sim 1,000 \text{ mm}^3$ , we observed that control tumors reached that size in  $\sim 25$  d, irradiated tumors in 28 d, T reg cell-depleted tumors in 32 d, and tumor treated with the combination needed a mean of 39 d (Fig. 7 D). Histological examination of tumors collected from the various groups 2 wk after treatment showed a significantly larger area of necrosis with the combination treatment than either of the single treatments and increased cleaved-caspase 3 staining in healthy areas of the tumor (Fig. 7 E and not depicted). In addition, tumors in the combination treatment group displayed a significant increase in the number of macrophages by double immunohistochemical staining with CD45 and Iba-1 markers (Fig. 7 F), as well as increase in CSF-1<sup>+</sup> tumor-infiltrating leukocytes, as determined by flow cytometry (not depicted). The differences observed in tumor growth translated to a very significant

increase in mouse survival, with mice treated with the combination therapy living almost twice as long as the control, untreated mice (Fig. 7 G). Interestingly, lung metastatic burden analyzed in a time-matched manner was not affected by local radiation treatment, and it was not significantly improved by the combination therapy over the T reg cell ablation treatment alone, at least at the time of analysis (Fig. 7 H), suggesting that transient T reg cell ablation alone is effective at limiting distant metastasis.

### DISCUSSION

Recent progress of immune-based cancer therapies is best exemplified by the clinical trials of CTLA4 blockade for the treatment of melanoma (Hodi et al., 2010) and by targeting PD-1 and PD-L1 in melanoma, renal cell carcinoma, and non-small cell lung and ovarian cancer (Brahmer et al., 2012; Topalian et al., 2012b). These interventions yield durable responses, but only in a limited fraction of recipients. Mechanistic studies in an oncogene-driven prostate cancer model showed that the therapeutic efficacy of monoclonal antibody-mediated checkpoint blockade depends on prior vaccination with cytokine-expressing tumor cells (Hurwitz et al., 2000). This finding, along with the observed clinical response rates of monotherapy checkpoint blockade in human trials, suggests that relieving the negative regulation exerted by these pathways alone is insufficient to attain potent anti-tumor immunity. Hence, combinatorial therapy of immunostimulatory antibodies has been proposed to increase response rates, with the potential risk of increasing dangerous side effects (Curran et al., 2010; Ascierto et al., 2013). In agreement with several studies in mouse models of experimental cancer, we found that as a single therapy, checkpoint blockade does not hinder primary tumor progression in a murine orthotopic model of oncogene-driven mammary carcinogenesis. However, efficient ablation of T reg cells alone achieved a significant reduction in tumor burden without the need for additional manipulation, revealing the essential role of T reg cells in oncogene-driven tumor growth. Consistent with these results, high tumor effector T cell to T reg cell ratio correlates with better tumor prognosis and clinical benefit of immunotherapy (Sato et al., 2005; Quezada et al., 2006; Balachandran et al., 2011). T reg cell ablation resulted in a sharply augmented expression of IFN- $\gamma$  by tumor-infiltrating T cells, which was necessary for the observed determent of tumor progression. The role of IFN- $\gamma$  in this model is consistent with its previously demonstrated role in immune surveillance of carcinogen-induced sarcomas and spontaneous epithelial carcinomas (Kaplan et al., 1998; Shankaran et al., 2001). Cytotoxic CD8<sup>+</sup> T cells, as well as NK cells, were not necessary, whereas CD4<sup>+</sup> T cells were required for anti-tumoral effect of T reg cell-mediated ablation. These results imply that IFN- $\gamma$  production by NK or CD8<sup>+</sup> T cells is dispensable for the anti-tumoral effect of T reg cell ablation, and they point to a potential role for CD4<sup>+</sup> T cells as a nonredundant source of protective IFN- $\gamma$  in PyMT breast carcinomas. CD4<sup>+</sup> T cells can exert IFN- $\gamma$ -dependent as well as direct cytotoxic effects on tumors cells (Shankaran et al., 2001; Quezada et al., 2010).

Increased IFN- $\gamma$  levels can contribute to the reduction of tumor growth by regulating the properties of tumor-infiltrating macrophages (O'Sullivan et al., 2012). In this regard, the observed sharp increase in expression of iNOS and proinflammatory chemokine expression by tumor-infiltrating myeloid cells raises the possibility that the therapeutic effect of T reg cell ablation is due to modulation of the accessory functions of tumor-infiltrating macrophages. The latter has been found to be essential for lung metastases in the MMTV-PyMT model (DeNardo et al., 2009).

In contrast to T reg cell ablation, anti-tumoral effect of both systemic and local administration of CTLA-4 neutralizing antibody is CD8<sup>+</sup> T cell dependent but CD4<sup>+</sup> T cell independent (van Elsas et al., 2001; Fransen et al., 2013). Likewise, the therapeutic effects of PD-1/PD-L1 blockade in chronic viral infection, and likely in cancer, are dependent on restoration of cytolytic responses and IFN- $\gamma$  production by CD8<sup>+</sup> T cells (Barber et al., 2006; Topalian et al., 2012a). The latter observations in combination with a dispensable role of CD8<sup>+</sup> T cells for the therapeutic benefit of T reg cell targeting offer a likely explanation for the failure of PD-1/PD-L1 blockade to mount biological response in our experiments.

CTLA-4 is expressed by T reg cells and is required for their function (Wing et al., 2008). Elegant genetic studies demonstrated that targeting CTLA-4 in both effector and T reg cell subsets affords the maximal inhibition of tumor growth in a transplantable B16 melanoma model (Peggs et al., 2009). Considering these findings, our study raises the possibility that the success of the PD-1 and CTLA-4 checkpoint blockade may be primarily due to selective (or relative) depletion or functional impairment of T reg cells. This is consistent with the recent studies suggesting that anti-CTLA-4 therapy works primarily through macrophage-mediated T reg cell depletion (Selby et al., 2013; Simpson et al., 2013). Additionally, PD-1/PD-L1 pathway blockade has also been shown to diminish T reg cell suppressor function (Wang et al., 2009).

Although CTLA-4 blockade did not affect lung metastatic burden, PD-1/PD-L1 blockage significantly diminished the number of metastatic foci in the lungs. The reduction, albeit markedly less pronounced than the one achieved through T reg cell ablation, is suggestive of a specific role for PD-1/PD-L1 inhibitory pathway in the colonization of lungs by disseminated single cancer cells. The observed selective role for PD-1 in lung metastasis was consistent with its prominent role in blocking lung inflammation, i.e., pneumonitis resulting from PD-1/PD-L1 deficiency, and clinical responses of PD-1 blockade in non-small cell lung cancer patients (Lucas et al., 2008; Brahmer et al., 2012; Topalian et al., 2012b).

Immune therapeutic approaches, such as checkpoint blockade and T reg cell depletion, can lead to the breaking of immune self-tolerance, inducing a variety of side effects that include rash, colitis, hepatitis, and endocrinopathies (Postow et al., 2012). Moreover, sustained ablation of T reg cells leads to a fatal lymphoproliferative syndrome (Kim et al., 2007, 2009). We found that transient T reg cell ablation does not have a significant effect on the overall mouse health status, as indicated

by normal mouse activity and weight, and minimal tissue immunopathology. These results bring hope to future translational studies, and they highlight the importance of developing methods of highly effective yet short-term T reg cell depletion that minimizes side effects.

Ionizing radiation therapy is widely used for the management of breast cancer due to its ability to induce cell death and proliferation arrest. In addition, radiotherapy can promote antigen presentation due to antigen and tissue damage signal release by dying cancer cells and reduce tolerance induction due to reduction of the tumor mass (Formenti and Demaria, 2009). Specific rationale for combined radiation and T reg cell ablation therapies is based on the known relative radioresistance of T reg cells (Komatsu and Hori, 2007). Our studies demonstrate that ablation of T reg cells during the course of radiotherapy significantly improves the outcome of treatment, not only by reducing tumor growth and metastasis but also by prolonging survival.

Altogether, our observations put forward the notion that targeting T reg cells is likely to result in pronounced clinical responses in breast cancer patients. Modulating this central mechanism of immune tolerance may expand the use of immunotherapy to tumor types which, like breast cancer, are not inherently immunogenic. Furthermore, current clinical outcomes might be significantly improved by combination of T reg cell depletion strategies with radiation, and possibly chemotherapy or targeted therapies against molecular drivers of oncogenesis.

## MATERIALS AND METHODS

**Mice.** *Foxp3<sup>DTTR</sup>* mice were generated in our laboratory and previously described (Kim et al., 2007).  $\beta 2M^{-/-}$  mice were purchased from Taconic. Mice bearing the MMTV-rTA and TetO-PyMT:IRES:Luc transgenes were provided by H. Varmus (National Cancer Institute, National Institutes of Health, Bethesda, MD). C57BL/6 MMTV-PyMT mice were a gift from M.O. Li (Memorial Sloan-Kettering Cancer Center, New York, NY). All animal studies were performed in accordance with an IACUC-approved protocol at the Memorial Sloan-Kettering Cancer Center.

**Animal experiments.** For oncogene induction, mice were placed on doxycycline-impregnated food pellets (625 ppm; Harlan-Teklad). For T reg cell ablation studies, DT (Sigma-Aldrich) was injected intravenously at 50 or 25  $\mu$ g per kg of body weight at indicated times. Mammary tumorigenic cell lines were generated via enzymatic dissociation of invasive tumors from MMTV-PyMT mice, expanded in Dulbecco's modified Eagle's medium and high glucose medium supplemented with 10% FBS, and transduced with a Firefly Luciferase retroviral vector using standard techniques. For orthotopic implantation studies, 100,000 cells were resuspended in PBS and mixed in a 1:1 ratio with growth factor-reduced Matrigel (BD), and injected in the mammary fat pad of isoflurane-anesthetized mice. Primary tumor outgrowth was monitored daily by taking measurements of the tumor length (*L*) and width (*W*). Tumor volume was calculated as  $\pi LW^2/6$ . For experimental lung metastasis assays, 500,000 cells were resuspended in PBS and inoculated via tail vein injection. Lung metastatic burden was quantified by counting the number of metastatic nodules under a dissection scope (Olympus), ex vivo bioluminescence using an IVIS200 imager (Xenogen), or calculating the ratio between the area covered by metastasis over the total area of the lung in histological sections. CTLA-4 (clone 9D9), PD-1 (clone RPM1-14), and PD-L1 (clone 10F.9G2) antibodies were administered i.p. at days 0, 3, and 6 at a dose of 100, 250, and 100  $\mu$ g per mouse, respectively, as indicated in the text. IFN- $\gamma$  (clone XMG1.2), NK cells (clone PK136), and CD4<sup>+</sup> (clone GK1.5) and CD8<sup>+</sup> (clone 2.43) T cell depletion was achieved through i.p.

injection of 1 mg and 300, 100, and 250  $\mu\text{g}$ , respectively, together with the second dose of DT (IFN- $\gamma$ , CD4, and NK) or 4 d after DT injection (CD8). All antibodies for animal studies were obtained from Bio X Cell. Radiation was administered in a single fraction of 12Gy when tumors reached a volume of  $\sim 100$  or  $250 \text{ mm}^3$  using an X-RAD 225Cx micro-irradiator. In brief, individual mice were anesthetized using isoflurane and positioned on a platform where a cone-beam CT imaging of the animal was performed to allow targeting the radiation field to the tumor, avoiding normal structures.

**Cytokine array.** Cytokines and chemokines were measured using a multiplex Luminex bead assay (Millipore). Tumors were lysed in buffer containing 50 mM Tris, 150 mM NaCl, 1% NP-40, 1 mM EDTA, and protease inhibitors. Cleared lysates were quantified and extracts bearing 20  $\mu\text{g}$  of total protein were incubated with mouse cytokine/chemokine magnetic bead panels I, II, and III from Milliplex, according to the manufacturer's instructions.

**Histology.** For histological analysis, tissues were fixed in 10% neutral buffered formalin and routinely processed for hematoxylin and eosin staining. Apoptosis (cleaved-caspase 3), proliferation (Ki67), leukocyte (CD45), and macrophage (IBA1) stainings were performed using automated IHC techniques by the Molecular Cytology Core Facility, and quantified using MetaMorph analysis.

**Flow cytometry.** Tumor-infiltrating lymphocytes were isolated by enzymatic dissociation of tumors using Liberase TL (Roche) and digested for 25 min, followed by Percoll (VWR) centrifugation to eliminate dead cells. Intracellular Foxp3 staining was performed using a Foxp3 mouse T reg cell staining kit (eBioscience). Cytokine staining was performed after stimulation of splenocytes or isolated TILs with 50 ng/ml PMA and 500 ng/ml ionomycin for 4–5 h in the presence of Golgi-Plug (BD). All antibodies used for flow cytometry staining were purchased from eBioscience, BioLegend, or BD. Stained cells were analyzed in a LSRII flow cytometer (BD). Data were analyzed using FlowJo software (Tree Star).

**FACS isolation and quantitative PCR analysis.** For qPCR analysis, tumors were processed by enzymatic digestion as previously described and myeloid or T cells were sorted based on their surface expression of CD45, TCR- $\beta$ , CD11B, and Gr1 using a FACSria II (BD). Sorted cells were lysed in TRIzol reagent (Invitrogen) and reverse-transcribed using SuperScript III Reverse transcription (Invitrogen). Semi-quantitative PCR was performed in an ABI Prism 7900HT instrument (Applied Biosystems) using SybrGreen PCR master mix (Applied Biosystems) and the following primers:  $\beta$ -actin forward, 5'-CTAAGGCCAACCGTGAAG-3';  $\beta$ -actin reverse, 5'-ACCAGAGGCATACAGGGACA-3'; IFN- $\gamma$  forward, 5'-ATCTG-GAGGAAGTGGCAAAA-3'; IFN- $\gamma$  reverse, 5'-TTCAAGACTTCAAA-GAGTCTGAGGTA-3'; CXCL9 forward, 5'-TTTTCTTTTGGG-CATCATCTT-3'; CXCL9 reverse, 5'-AGCATCGTCATTCCTTA-TCACT-3'; CXCL10 forward, 5'-GAAATCATCCCTGCGAGCCT-3'; CXCL10 reverse, 5'-TTGATGGTCTTAGATTCGGATTTC-3'; iNOS forward, 5'-CTTTGCCACGGACGAC-3'; and iNOS reverse, 5'-TCAT-TGTACTCTGAGGGCTGAC-3'.

**Statistical analysis.** All statistical analysis was performed using Student's *t* test or ANOVA analysis as indicated with Prism software (GraphPad Software).

We thank Drs. Harold Varmus and Ming Li for providing TOMT mice and C57BL/6 MMTV-PyMT mice, respectively.

This work was supported by a fellowship from the American Cancer Society (P.D. Bos), National Institutes of Health (NIH) Immunology Training grant T32CA009149-37 (P.D. Bos), a Geoffrey Beene Metastasis Center Grant Award (A.Y. Rudensky), and NIH grant R37 AI034206 and Ludwig Center at Memorial Sloan-Kettering Cancer Center (A.Y. Rudensky). A.Y. Rudensky is an investigator with the Howard Hughes Medical Institute. The authors declare no competing financial interests.

Submitted: 12 April 2013

Accepted: 11 September 2013

## REFERENCES

- Ascierto, P.A., M. Kalos, D.A. Schaer, M.K. Callahan, and J.D. Wolchok. 2013. Biomarkers for immunostimulatory monoclonal antibodies in combination strategies for melanoma and other tumor types. *Clin. Cancer Res.* 19:1009–1020. <http://dx.doi.org/10.1158/1078-0432.CCR-12-2982>
- Balachandran, V.P., M.J. Cavnar, S. Zeng, Z.M. Bamboat, L.M. Ocuin, H. Obaid, E.C. Sorenson, R. Popow, C. Ariyan, F. Rossi, et al. 2011. Imatinib potentiates antitumor T cell responses in gastrointestinal stromal tumor through the inhibition of Ido. *Nat. Med.* 17:1094–1100. <http://dx.doi.org/10.1038/nm.2438>
- Barber, D.L., E.J. Wherry, D. Masopust, B. Zhu, J.P. Allison, A.H. Sharpe, G.J. Freeman, and R. Ahmed. 2006. Restoring function in exhausted CD8 T cells during chronic viral infection. *Nature.* 439:682–687. <http://dx.doi.org/10.1038/nature04444>
- Brahmer, J.R., S.S. Tykodi, L.Q. Chow, W.J. Hwu, S.L. Topalian, P. Hwu, C.G. Drake, L.H. Camacho, J. Kauh, K. Odunsi, et al. 2012. Safety and activity of anti-PD-L1 antibody in patients with advanced cancer. *N. Engl. J. Med.* 366:2455–2465. <http://dx.doi.org/10.1056/NEJMoa1200694>
- Chen, L., and D.B. Flies. 2013. Molecular mechanisms of T cell co-stimulation and co-inhibition. *Nat. Rev. Immunol.* 13:227–242. <http://dx.doi.org/10.1038/nri3405>
- Coussens, L.M., L. Zitvogel, and A.K. Palucka. 2013. Neutralizing tumor-promoting chronic inflammation: a magic bullet? *Science.* 339:286–291. <http://dx.doi.org/10.1126/science.1232227>
- Curran, M.A., W. Montalvo, H. Yagita, and J.P. Allison. 2010. PD-1 and CTLA-4 combination blockade expands infiltrating T cells and reduces regulatory T and myeloid cells within B16 melanoma tumors. *Proc. Natl. Acad. Sci. USA.* 107:4275–4280. <http://dx.doi.org/10.1073/pnas.0915174107>
- Demaria, S., N. Kawashima, A.M. Yang, M.L. Devitt, J.S. Babb, J.P. Allison, and S.C. Formenti. 2005. Immune-mediated inhibition of metastases after treatment with local radiation and CTLA-4 blockade in a mouse model of breast cancer. *Clin. Cancer Res.* 11:728–734.
- DeNardo, D.G., J.B. Barreto, P. Andreu, L. Vazquez, D. Tawfik, N. Kolhatkar, and L.M. Coussens. 2009. CD4(+) T cells regulate pulmonary metastasis of mammary carcinomas by enhancing protumor properties of macrophages. *Cancer Cell.* 16:91–102. <http://dx.doi.org/10.1016/j.ccr.2009.06.018>
- Drake, C.G. 2012. Combination immunotherapy approaches. *Ann. Oncol.* 23:viii41–6. <http://dx.doi.org/10.1093/annonc/mds262>
- Facciabene, A., G.T. Motz, and G. Coukos. 2012. T-regulatory cells: key players in tumor immune escape and angiogenesis. *Cancer Res.* 72:2162–2171. <http://dx.doi.org/10.1158/0008-5472.CAN-11-3687>
- Formenti, S.C., and S. Demaria. 2009. Systemic effects of local radiotherapy. *Lancet Oncol.* 10:718–726. [http://dx.doi.org/10.1016/S1470-2045\(09\)70082-8](http://dx.doi.org/10.1016/S1470-2045(09)70082-8)
- Fransen, M.F., T.C. van der Sluis, F. Ossendorp, R. Arens, and C.J. Melief. 2013. Controlled Local Delivery of CTLA-4 Blocking Antibody Induces CD8+ T-Cell-Dependent Tumor Eradication and Decreases Risk of Toxic Side Effects. *Clin. Cancer Res.* In press.
- Gasteiger, G., S. Hemmers, M.A. Firth, A. Le Floch, M. Huse, J.C. Sun, and A.Y. Rudensky. 2013. IL-2-dependent tuning of NK cell sensitivity for target cells is controlled by regulatory T cells. *J. Exp. Med.* 210:1167–1178. <http://dx.doi.org/10.1084/jem.20122462>
- Guy, C.T., R.D. Cardiff, and W.J. Muller. 1992. Induction of mammary tumors by expression of polyomavirus middle T oncogene: a transgenic mouse model for metastatic disease. *Mol. Cell. Biol.* 12:954–961.
- Heimann, R., and S. Hellman. 2000. Clinical progression of breast cancer malignant behavior: what to expect and when to expect it. *J. Clin. Oncol.* 18:591–599.
- Hodi, F.S., S.J. O'Day, D.F. McDermott, R.W. Weber, J.A. Sosman, J.B. Haanen, R. Gonzalez, C. Robert, D. Schadendorf, J.C. Hassel, et al. 2010. Improved survival with ipilimumab in patients with metastatic melanoma. *N. Engl. J. Med.* 363:711–723. <http://dx.doi.org/10.1056/NEJMoa1003466>
- Hurwitz, A.A., B.A. Foster, E.D. Kwon, T. Truong, E.M. Choi, N.M. Greenberg, M.B. Burg, and J.P. Allison. 2000. Combination immunotherapy of primary prostate cancer in a transgenic mouse model using CTLA-4 blockade. *Cancer Res.* 60:2444–2448.



- Kaplan, D.H., V. Shankaran, A.S. Dighe, E. Stockert, M. Aguet, L.J. Old, and R.D. Schreiber. 1998. Demonstration of an interferon gamma-dependent tumor surveillance system in immunocompetent mice. *Proc. Natl. Acad. Sci. USA*. 95:7556–7561. <http://dx.doi.org/10.1073/pnas.95.13.7556>
- Kim, J.M., J.P. Rasmussen, and A.Y. Rudensky. 2007. Regulatory T cells prevent catastrophic autoimmunity throughout the lifespan of mice. *Nat. Immunol.* 8:191–197. <http://dx.doi.org/10.1038/ni1428>
- Kim, J., K. Lahl, S. Hori, C. Loddenkemper, A. Chaudhry, P. deRoos, A. Rudensky, and T. Sparwasser. 2009. Cutting edge: depletion of Foxp3+ cells leads to induction of autoimmunity by specific ablation of regulatory T cells in genetically targeted mice. *J. Immunol.* 183:7631–7634. <http://dx.doi.org/10.4049/jimmunol.0804308>
- Klages, K., C.T. Mayer, K. Lahl, C. Loddenkemper, M.W. Teng, S.F. Ngiew, M.J. Smyth, A. Hamann, J. Huehn, and T. Sparwasser. 2010. Selective depletion of Foxp3+ regulatory T cells improves effective therapeutic vaccination against established melanoma. *Cancer Res.* 70:7788–7799. <http://dx.doi.org/10.1158/0008-5472.CAN-10-1736>
- Komatsu, N., and S. Hori. 2007. Full restoration of peripheral Foxp3+ regulatory T cell pool by radioresistant host cells in scurfy bone marrow chimeras. *Proc. Natl. Acad. Sci. USA*. 104:8959–8964. <http://dx.doi.org/10.1073/pnas.0702004104>
- Li, X., E. Kostareli, J. Suffner, N. Garbi, and G.J. Hämmerling. 2010. Efficient Treg depletion induces T-cell infiltration and rejection of large tumors. *Eur. J. Immunol.* 40:3325–3335. <http://dx.doi.org/10.1002/eji.201041093>
- Lin, E.Y., J.G. Jones, P. Li, L. Zhu, K.D. Whitney, W.J. Muller, and J.W. Pollard. 2003. Progression to malignancy in the polyoma middle T oncoprotein mouse breast cancer model provides a reliable model for human diseases. *Am. J. Pathol.* 163:2113–2126. [http://dx.doi.org/10.1016/S0002-9440\(10\)63568-7](http://dx.doi.org/10.1016/S0002-9440(10)63568-7)
- Lucas, J.A., J. Menke, W.A. Rabacal, F.J. Schoen, A.H. Sharpe, and V.R. Kelley. 2008. Programmed death ligand 1 regulates a critical checkpoint for autoimmune myocarditis and pneumonitis in MRL mice. *J. Immunol.* 181:2513–2521.
- Minn, A.J., G.P. Gupta, D. Padua, P. Bos, D.X. Nguyen, D. Nuyten, B. Kreike, Y. Zhang, Y. Wang, H. Ishwaran, et al. 2007. Lung metastasis genes couple breast tumor size and metastatic spread. *Proc. Natl. Acad. Sci. USA*. 104:6740–6745. <http://dx.doi.org/10.1073/pnas.0701138104>
- Mokyr, M.B., T. Kalinichenko, L. Gorelik, and J.A. Bluestone. 1998. Realization of the therapeutic potential of CTLA-4 blockade in low-dose chemotherapy-treated tumor-bearing mice. *Cancer Res.* 58:5301–5304.
- O'Sullivan, T., R. Saddawi-Konefka, W. Vermi, C.M. Koebel, C. Arthur, J.M. White, R. Uppaluri, D.M. Andrews, S.F. Ngiew, M.W. Teng, et al. 2012. Cancer immunoediting by the innate immune system in the absence of adaptive immunity. *J. Exp. Med.* 209:1869–1882. <http://dx.doi.org/10.1084/jem.20112738>
- Pardoll, D.M. 2012. The blockade of immune checkpoints in cancer immunotherapy. *Nat. Rev. Cancer.* 12:252–264. <http://dx.doi.org/10.1038/nrc3239>
- Peggs, K.S., S.A. Quezada, C.A. Chambers, A.J. Korman, and J.P. Allison. 2009. Blockade of CTLA-4 on both effector and regulatory T cell compartments contributes to the antitumor activity of anti-CTLA-4 antibodies. *J. Exp. Med.* 206:1717–1725. <http://dx.doi.org/10.1084/jem.20082492>
- Podsypanina, K., K. Politi, L.J. Beverly, and H.E. Varmus. 2008. Oncogene cooperation in tumor maintenance and tumor recurrence in mouse mammary tumors induced by Myc and mutant Kras. *Proc. Natl. Acad. Sci. USA*. 105:5242–5247. <http://dx.doi.org/10.1073/pnas.0801197105>
- Postow, M.A., J. Harding, and J.D. Wolchok. 2012. Targeting immune checkpoints: releasing the restraints on anti-tumor immunity for patients with melanoma. *Cancer J.* 18:153–159. <http://dx.doi.org/10.1097/PPO.0b013e318250c001>
- Quezada, S.A., K.S. Peggs, M.A. Curran, and J.P. Allison. 2006. CTLA4 blockade and GM-CSF combination immunotherapy alters the intratumor balance of effector and regulatory T cells. *J. Clin. Invest.* 116:1935–1945. <http://dx.doi.org/10.1172/JCI27745>
- Quezada, S.A., T.R. Simpson, K.S. Peggs, T. Merghoub, J. Vider, X. Fan, R. Blasberg, H. Yagita, P. Muranski, P.A. Antony, et al. 2010. Tumor-reactive CD4+ T cells develop cytotoxic activity and eradicate large established melanoma after transfer into lymphopenic hosts. *J. Exp. Med.* 207:637–650. <http://dx.doi.org/10.1084/jem.20091918>
- Sato, E., S.H. Olson, J. Ahn, B. Bundy, H. Nishikawa, F. Qian, A.A. Jungbluth, D. Frosina, S. Gnjatic, C. Ambrosone, et al. 2005. Intraepithelial CD8+ tumor-infiltrating lymphocytes and a high CD8+/regulatory T cell ratio are associated with favorable prognosis in ovarian cancer. *Proc. Natl. Acad. Sci. USA*. 102:18538–18543. <http://dx.doi.org/10.1073/pnas.0509182102>
- Schreiber, R.D., L.J. Old, and M.J. Smyth. 2011. Cancer immunoediting: integrating immunity's roles in cancer suppression and promotion. *Science*. 331:1565–1570. <http://dx.doi.org/10.1126/science.1203486>
- Selby, M.J., J.J. Engelhardt, M. Quigley, K.A. Henning, T. Chen, M. Srinivasan, and A.J. Korman. 2013. Anti-CTLA-4 Antibodies of IgG2a Isotype Enhance Antitumor Activity through Reduction of Intratumoral Regulatory T Cells. *Cancer Immunology Research*. 1:32–42. <http://dx.doi.org/10.1158/2326-6066.CIR-13-0013>
- Shankaran, V., H. Ikeda, A.T. Bruce, J.M. White, P.E. Swanson, L.J. Old, and R.D. Schreiber. 2001. IFN $\gamma$  and lymphocytes prevent primary tumour development and shape tumour immunogenicity. *Nature*. 410:1107–1111. <http://dx.doi.org/10.1038/35074122>
- Simpson, T.R., F. Li, W. Montalvo-Ortiz, M.A. Sepulveda, K. Bergerhoff, F. Arce, C. Roddie, J.Y. Henry, H. Yagita, J.D. Wolchok, et al. 2013. Fc-dependent depletion of tumor-infiltrating regulatory T cells co-defines the efficacy of anti-CTLA-4 therapy against melanoma. *J. Exp. Med.* 210:1695–1710. <http://dx.doi.org/10.1084/jem.20130579>
- Strome, S.E., H. Dong, H. Tamura, S.G. Voss, D.B. Flies, K. Tamada, D. Salomao, J. Cheville, F. Hirano, W. Lin, et al. 2003. B7-H1 blockade augments adoptive T-cell immunotherapy for squamous cell carcinoma. *Cancer Res.* 63:6501–6505.
- Tan, W., W. Zhang, A. Strasner, S. Grivennikov, J.Q. Cheng, R.M. Hoffman, and M. Karin. 2011. Tumour-infiltrating regulatory T cells stimulate mammary cancer metastasis through RANKL-RANK signaling. *Nature*. 470:548–553. <http://dx.doi.org/10.1038/nature09707>
- Teng, M.W., S.F. Ngiew, B. von Scheidt, N. McLaughlin, T. Sparwasser, and M.J. Smyth. 2010. Conditional regulatory T-cell depletion releases adaptive immunity preventing carcinogenesis and suppressing established tumor growth. *Cancer Res.* 70:7800–7809. <http://dx.doi.org/10.1158/0008-5472.CAN-10-1681>
- Topalian, S.L., C.G. Drake, and D.M. Pardoll. 2012a. Targeting the PD-1/B7-H1 (PD-L1) pathway to activate anti-tumor immunity. *Curr. Opin. Immunol.* 24:207–212. <http://dx.doi.org/10.1016/j.coi.2011.12.009>
- Topalian, S.L., F.S. Hodi, J.R. Brahmer, S.N. Gettinger, D.C. Smith, D.F. McDermott, J.D. Powderly, R.D. Carvajal, J.A. Sosman, M.B. Atkins, et al. 2012b. Safety, activity, and immune correlates of anti-PD-1 antibody in cancer. *N. Engl. J. Med.* 366:2443–2454. <http://dx.doi.org/10.1056/NEJMoa1200690>
- van Elsas, A., A.A. Hurwitz, and J.P. Allison. 1999. Combination immunotherapy of B16 melanoma using anti-cytotoxic T lymphocyte-associated antigen 4 (CTLA-4) and granulocyte/macrophage colony-stimulating factor (GM-CSF)-producing vaccines induces rejection of subcutaneous and metastatic tumors accompanied by autoimmune depigmentation. *J. Exp. Med.* 190:355–366. <http://dx.doi.org/10.1084/jem.190.3.355>
- van Elsas, A., R.P. Sutmoller, A.A. Hurwitz, J. Ziskin, J. Villasenor, J.P. Medema, W.W. Overwijk, N.P. Restifo, C.J. Melief, R. Offringa, and J.P. Allison. 2001. Elucidating the autoimmune and antitumor effector mechanisms of a treatment based on cytotoxic T lymphocyte antigen-4 blockade in combination with a B16 melanoma vaccine: comparison of prophylaxis and therapy. *J. Exp. Med.* 194:481–489. <http://dx.doi.org/10.1084/jem.194.4.481>
- Waitz, R., S.B. Solomon, E.N. Petre, A.E. Trumble, M. Fassò, L. Norton, and J.P. Allison. 2012. Potent induction of tumor immunity by combining tumor cryoablation with anti-CTLA-4 therapy. *Cancer Res.* 72:430–439. <http://dx.doi.org/10.1158/0008-5472.CAN-11-1782>
- Wang, W., R. Lau, D. Yu, W. Zhu, A. Korman, and J. Weber. 2009. PD1 blockade reverses the suppression of melanoma antigen-specific CTL by CD4+ CD25(Hi) regulatory T cells. *Int. Immunol.* 21:1065–1077. <http://dx.doi.org/10.1093/intimm/dxp072>
- Willimsky, G., and T. Blankenstein. 2005. Sporadic immunogenic tumours avoid destruction by inducing T-cell tolerance. *Nature*. 437:141–146. <http://dx.doi.org/10.1038/nature03954>
- Wing, K., Y. Onishi, P. Prieto-Martin, T. Yamaguchi, M. Miyara, Z. Fehervari, T. Nomura, and S. Sakaguchi. 2008. CTLA-4 control over Foxp3+ regulatory T cell function. *Science*. 322:271–275. <http://dx.doi.org/10.1126/science.1160062>